

Article

Regulatory Networks of Flowering Genes in *Angelica sinensis* during Vernalization

Mimi Luo ^{1†}, Xiaoxia Liu ^{1†}, Hongyan Su ¹, Meiling Li ¹, Mengfei Li ^{1*} and Jianhe Wei ^{2,*}

¹ State Key Laboratory of Aridland Crop Science, College of Life Science and Technology, Gansu Agricultural University, Lanzhou 730070, China; luomimi9521@163.com (M.L.); 18893481962@163.com (X.L.); shy922322@163.com (H.S.); mlli1996@163.com (M.L.)

² Institute of Medicinal Plant Development, Chinese Academy of Medical Sciences & Peking Union Medical College, Beijing 100193, China

* Correspondence: lmf@gsau.edu.cn (M.L.); jhwei@implad.ac.cn (J.W.)

† These authors contributed equally to this work.

Abstract: *Angelica sinensis* is a low-temperature and long-day perennial herb that has been widely used for cardio-cerebrovascular diseases in recent years. In commercial cultivation, up to 40% of flowering decreases the officinal yield of roots and accumulation of bioactive compounds. Although the regulatory mechanism of flowering genes during the photoperiod has been revealed, the networks during vernalization have not been mapped. Here, transcriptomics profiles of *A. sinensis* with uncompleted (T1), completed (T2) and avoided vernalization (T3) were performed using RNA-seq, and genes expression was validated with qRT-PCR. A total of 61,241 isoforms were annotated on KEGG, KOG, Nr and Swiss-Prot databases; 4212 and 5301 differentially expressed genes (DEGs) were observed; and 151 and 155 genes involved in flowering were dug out at T2 vs. T1 and T3 vs. T1, respectively. According to functional annotation, 104 co-expressed genes were classified into six categories: FLC expression (22; e.g., *VILs*, *FCA* and *FLK*), sucrose metabolism (12; e.g., *TPSs*, *SUS3* and *SPSs*), hormone response (18; e.g., *GID1B*, *RAP2s* and *IAAs*), circadian clock (2; i.e., *ELF3* and *COR27*), downstream floral integrators and meristem identity (15; e.g., *SOC1*, *AGL65* and *SPLs*) and cold response (35; e.g., *PYLs*, *ERFs* and *CORs*). The expression levels of candidate genes were almost consistent with FPKM values and changes in sugar and hormone contents. Based on their functions, four pathways that regulate flowering during vernalization were mapped, including the vernalization pathway, the autonomic pathway, the age pathway and the GA (hormone) pathway. This transcriptomic analysis provides new insights into the gene-regulatory networks of flowering in *A. sinensis*.

Keywords: *Angelica sinensis*; vernalization; flowering; transcriptomic; gene-regulatory networks

Citation: Luo, M.; Liu, X.; Su, H.; Li, M.-L.; Li, M.-F.; Wei, J. Regulatory Networks of Flowering Genes in *Angelica sinensis* during Vernalization. *Plants* **2022**, *11*, 1355. <https://doi.org/10.3390/plants11101355>

Academic Editor: Chris Helliwell

Received: 2 April 2022

Accepted: 18 May 2022

Published: 19 May 2022

Publisher's Note: MDPI stays neutral with regard to jurisdictional claims in published maps and institutional affiliations.



Copyright: © 2022 by the authors. Licensee MDPI, Basel, Switzerland. This article is an open access article distributed under the terms and conditions of the Creative Commons Attribution (CC BY) license (<https://creativecommons.org/licenses/by/4.0/>).

1. Introduction

Angelica sinensis (Oliv.) Diels (Apiaceae, alt. Umbelliferae) is a perennial herbaceous species, originally native to China, with a dense population in Gansu province at an altitude of 2200–3000 m [1]. The roots have been widely used as a traditional Chinese herbal remedy in China, Korea and Japan for nourishing the blood, regulating menstrual disorders, relaxing bowels, etc., for over 2000 years [2,3]. Currently, over 50 compounds have been isolated from the roots, including phthalides, organic acids and polysaccharides, which confer pharmacological effects, including cardio-cerebrovascular, hepatoprotective, antioxidant, antispasmodic and immunomodulatory effects [4–6].

At present, over 43,500 ha of commercial of *A. sinensis* cultivation supplies the increasing market demand; however, up to 40% of flowering of plants in the field makes the roots lignified, decreasing the yield of roots and the accumulation bioactive compounds [7–9]. Previous studies have demonstrated that *A. sinensis* is a low-temperature

and long-day plant that must experience vernalization (0 to 5 °C) and long-day conditions (>12 h daylight) for the transition from vegetative growth to flowering [10]. Thereafter, the flowering could be effectively avoided after the seedlings stored below freezing temperature (<0 °C) [11–13] or significantly inhibited when the plants grew under sunshade at photoperiod [14].

To date, the gene regulatory mechanism of the flowering during the photoperiod has been shown, with upstream regulatory pathway genes (e.g., *CONSTANS* (*CO*), *FLOWERING LOCUS C* (*FLC*) and *PHYTOCHROME A* (*PHYA*)), downstream floral integrator genes (e.g., *FLOWERING LOCUS T* (*FT*), *SUPPRESSOR OF OVEREXPRESSION OF CONSTANS 1* (*SOC1*) and *FT-interacting protein 1* (*FTIP1*)), downstream floral meristem identity genes (e.g., *LEAFY* (*LFY*), *APETALA 1* (*AP1*) and *AP2*)), autonomous pathway genes (e.g., *flowering time control protein FCA* (*FCA*), *flowering time control protein FPA* (*FPA*) and *FY*), sucrose metabolism genes (e.g., *sucrose synthase* (*SUS*), *alpha-amylase* (*AMY*) and *glucan endo-1,3-b-glucosidase* (*GLU*)) and gibberellin (GA) pathway genes (e.g., *gibberellin 2-β-dioxygenase 1* (*GA2OX1*), *gibberellin 20-oxidase 1* (*GA20OX1*) and *DELLA protein GAI* (*GAI*)) [15–18]. Although physiological changes (e.g., soluble sugar, protein and hormones) during vernalization and freezing storage have been investigated [19,20], gene-regulatory networks involved in the flowering of *A. sinensis* during vernalization have not been mapped.

In the present study, the alterations of transcripts in *A. sinensis* with three different treatments, including uncompleted (T1), completed (T2) and avoided vernalization (T3) were analyzed by combining isoforms with Illumina sequencing, and 104 DEGs involved in flowering and cold response were observed. The changes in soluble sugar and hormones (GA₃, IAA and ABA) were examined via a spectrophotometer and HPLC.

2. Materials and Methods

2.1. Plant Material

The seedlings (root-tip size 0.4–0.5 cm; Figure S1) of *Angelica sinensis* (cultivar Mingui 1) were, respectively, stored at 0 and –3 °C on 21 October 2020. The seedlings stored at 0 °C were collected after 14 (T1) and 60 days (T2), and the seedlings stored at –3 °C were collected after 125 days (T3). The shoot apical meristem (SAM) of the collected seedlings was immediately frozen and stored in liquid nitrogen for transcriptomic analysis and qRT-PCR validation. Herein, T1 (0 °C 14 d), T2 (0 °C 60 d) and T3 (–3 °C 125 d) treatments represent uncompleted, completed and avoided vernalization, respectively (Figure S2).

2.2. Isoform Sequencing and Analysis

The total RNA of SAM was extracted using a Trizol reagent, the integrity of the RNA was determined using an Agilent 2100 Bioanalyzer and agarose gel electrophoresis, and the purity and concentration of the RNA were determined using a NanoDrop micro-spectrophotometer. mRNA was enriched by Oligo (dT) magnetic beads and then reverse-transcribed into cDNA using a Clontech SMARTer cDNA Synthesis Kit. The cDNA was amplified by PCR for 13 cycles to generate large-scale, double-stranded cDNA and then purified using AMPure XP beads to select cDNAs > 4 kb in size. SMRTbell library was constructed after the cDNAs were damage-repaired and end-repaired, and the sequencing adapters were ligated. The SMRTbell template was annealed to bind the primer and polymerase.

The raw reads of the cDNA library were sequenced on a Pacific Biosciences Sequel platform by Gene Denovo Biotechnology Co., Ltd. (Guangzhou, China), and then the raw reads were analyzed using a SMRT Link (V8.0.0) [21]. Briefly, high-quality circular consensus sequences (CCS) were extracted from the raw reads, and full-length non-chimeric (FLNC) reads were obtained by removing the primers, barcodes, poly (A) tail trimmings and concatemers. Then, the FLNC reads were clustered to generate the entire isoforms [22]. Similar FLNC reads were used, the minimap2 was used to cluster hierarchically to

obtain the consistency sequence (unpolished consensus isoforms), the quiver algorithm was used to further correct the consistency of the sequence and then high-quality isoforms were obtained with a prediction accuracy ≥ 0.99 . Finally, the full-length isoforms were analyzed and annotated against the databases using BLAST: NCBI non-redundant protein (Nr) (<http://www.ncbi.nlm.nih.gov>, accessed on 1 December 2021), Kyoto Encyclopedia of Genes and Genomes (KEGG) (<http://www.genome.jp/kegg>, accessed on 1 December 2021), Eukaryotic Orthologous Groups of proteins (KOG), Swiss-Prot (<https://www.uniprot.org>, accessed on 1 December 2021), Gene Ontology (GO) (<http://www.geneontology.org/>, accessed on 1 December 2021) and COG/KOG (<http://www.ncbi.nlm.nih.gov/COG>, accessed on 1 December 2021) with the BLASTx program (<http://www.ncbi.nlm.nih.gov/BLAST/>, accessed on 1 December 2021) at an E-value threshold of 1×10^{-5} to evaluate the sequence similarity with genes of other species.

2.3. Illumina Sequencing and DEGs Analysis

The procedures of total RNA extraction, integrity and purity determination, as well as cDNA library construction, for the samples T1, T2 and T3 were conducted according to the “Section 2.2” description. After the samples were sequenced, the raw reads were filtered using a FASTQ system to obtain high-quality clean reads [23] with the following parameters: removing reads containing adapters, removing reads containing more than 10% unknown nucleotides (N), and removing low-quality reads containing more than 50% low quality (Q-value ≤ 20) bases. The paired-end clean reads were mapped to the full-length isoforms using HISAT2. 2.4 to obtain the unique- and multiple-mapped reads [24] with “-rna-strandness RF” and other parameters set as a default.

The expression level of each transcript was normalized to the values of the fragments per kilobase of the exon model per million mapped reads (FPKM). Differential expression analysis of transcripts was performed using DESeq2 software [25] between different groups. The differential expression levels at T2 vs. T1 and T3 vs. T1 were determined with the criteria of the false discovery rate (FDR) < 0.05 and $|\log_2(\text{fold-change})| > 1$. To date, the genome of *A. sinensis* has not been reported to be sequenced and assembled. The function of DEGs was analyzed using BLAST against the full-length isoforms of *A. sinensis* based on the Nr, KEGG, KOG and Swiss-Prot databases.

For GO enrichment analysis, all DEGs were mapped to GO terms in the GO database, gene numbers were calculated (FDR ≤ 0.05) for every term, and GO terms that were significantly enriched in DEGs compared with the full-length isoforms of *A. sinensis* were defined using a hypergeometric test. For the KEGG pathway enrichment analysis, significantly enriched metabolic pathways or signal transduction pathways in DEGs compared with the full-length isoforms of *A. sinensis* were defined with FDR ≤ 0.05 as a threshold.

2.4. qRT-PCR Validation

The procedures of total RNA extraction, integrity and purity determination for the samples T1, T2 and T3 were conducted according to the description labeled “Section 2.2”. Primer sequences of selected DEGs (Table S1) were designed using an NCBI primer-blast tool and synthesized by Sangon Biotech (Shanghai, China). First-strand cDNA was synthesized using a FastKing RT kit (KR116; Tiangen, Beijing, China) with one cycle at 42 °C for 15 min and then at 95 °C for 3 min. qRT-PCR gene expression was carried out using a SuperReal PreMix Plus (SYBR Green) (FP205; Tiangen, Beijing, China) with one cycle at 95 °C for 15 min, followed by 40 cycles at 95 °C for 10 s, 60 °C for 20 s and 72 °C for 30 s. Melting curve analysis was performed after incubation at 95 °C for 15 s, 60 °C for 1 min and 95 °C for 1 s. The *actin* gene was used as a reference control gene [9,15,16,26]. Herein, the cycle threshold (Ct) values and standard curves of the *ACT* gene at different volumes (0.25, 0.5, 1.0, 1.5, 2.0 and 3.0 μL) were built to correct the gene expression level (Figures S3 and S4). The relative expression level (REL) of genes was calculated using a $2^{-\Delta\Delta C_t}$ method (Ct, cycle threshold value of target gene) [27].

2.5. Measurement of Soluble Sugar and Endogenous Hormones Contents

Soluble sugar content was measured using phenol-sulfuric acid [28]. Endogenous hormones (GA₃, IAA and ABA) contents were measured using a HPLC method [29].

2.6. Statistical Analysis

In order to obtain the precise estimation of PCR efficiency, each experiment for qRT-PCR validation was performed with three biological replicates, along with three technical replicates. Statistical analysis was performed via ANOVA and Duncan multiple comparison tests, and SPSS 22.0 was the software package used with $p < 0.05$ as the basis for statistical differences.

3. Results

3.1. Full-Length Isoform Analysis

A total of 1,031,219 high-fidelity reads were extracted after 33 full passes of raw reads, 76,840 polished high-quality isoforms were obtained using a Quiver calculation and 64,117 full-length isoforms were generated after the FLNC reads were clustered (Figure S5). A total of 61,241 isoforms were annotated on KEGG (60,792), KOG (42,645), Nr (61,161) and Swiss-Prot (51,070) databases (Figure 1A), and the top 10 species in terms of distribution against Nr, were *Daucus carota*, *Apium graveolens*, *Nyssa sinensis*, *Angelica sinensis*, *Petroselinum crispum*, *Camellia sinensis*, *Mikania micrantha*, *Vitis vinifera*, *Oliveria decumbens* and *Beta vulgaris* (Figure 1B). Since the genome of *A. sinensis* has not been sequenced, the isoforms are needed to compare with other species and the limited genes of *A. sinensis* in the NR database.

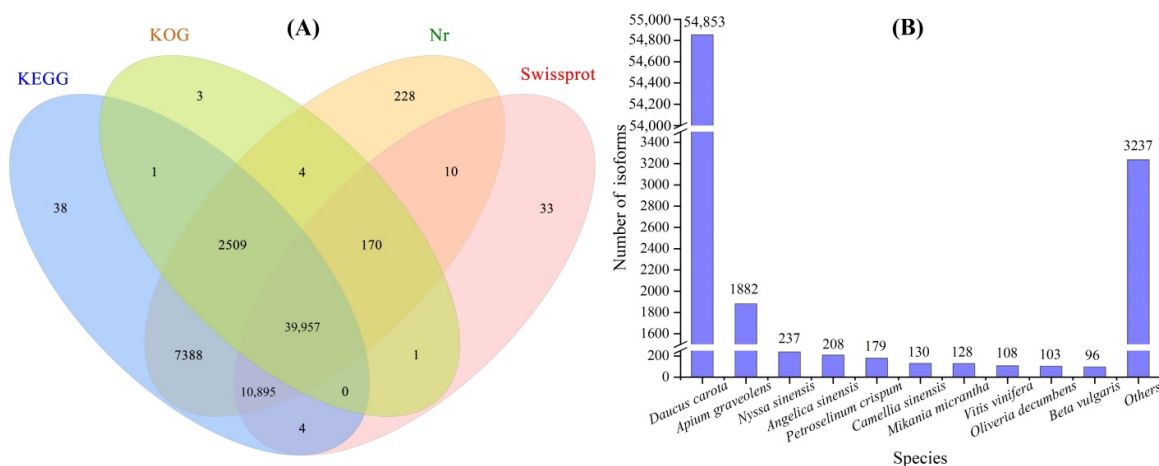


Figure 1. Basic annotation of full-length isoforms against KEGG, KOG, Nr and Swiss-Prot databases (A) and top 10 species in terms of distribution of the isoforms against Nr (B).

3.2. Illumina Sequencing of T1, T2 and T3

To reveal the molecular mechanisms responsible for regulating the flowering of *A. sinensis* during vernalization, a comparison of gene transcription in response to different temperatures and durations was performed. In this study, 9.14, 9.19 and 8.63 million raw reads were generated for T1, T2 and T3, respectively. After raw data filtering, 9.12, 9.16 and 8.61 million clean reads were collected. After mapping on the isoforms, 5.33, 5.50 and 5.23 million unique mapped reads, as well as 2.27, 2.31 and 2.05 million multiple mapped reads, were obtained from the T1, T2 and T3, respectively. Meanwhile, the exon rate of all the three treatments reached 100% (Table 1).

Table 1. Summary of Illumina sequencing data of *A. sinensis* for T1, T2 and T3.

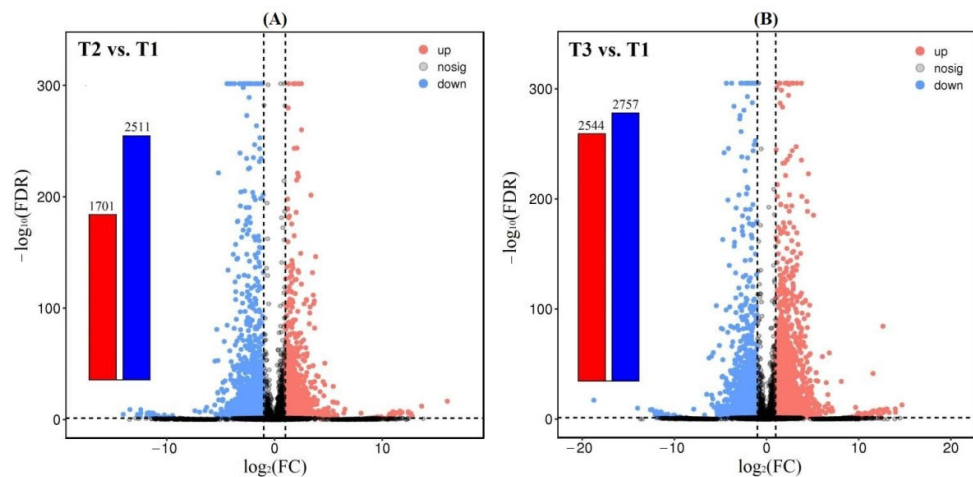
| | T1 | T2 | T3 |
|--|-------|-------|-------|
| Raw data | | | |
| Data of reads number (million) | 9.14 | 9.19 | 8.63 |
| Q20(%) | 97.87 | 97.87 | 97.99 |
| Q30(%) | 93.88 | 93.87 | 94.20 |
| GC (%) | 42.90 | 42.99 | 43.07 |
| Filtered data | | | |
| Data of reads number (million) | 9.12 | 9.16 | 8.61 |
| Q20 (%) | 97.97 | 97.97 | 98.09 |
| Q30 (%) | 94.01 | 94.10 | 94.34 |
| GC (%) | 42.85 | 42.94 | 43.01 |
| Mapped data against full-length isoform | | | |
| Data of unique mapped reads (million) | 5.33 | 5.50 | 5.23 |
| Data of multiple mapped reads (million) | 2.27 | 2.31 | 2.05 |
| Exon rate (%) | 100 | 100 | 100 |

Note: T1 (0 °C 14 d), uncompleted vernalization; T2 (0 °C 60 d), completed vernalization; T3 (−3 °C 125 d), avoided vernalization.

3.3. Analysis and Annotation of Differentially Expressed Genes (DEGs)

3.3.1. DEGs at T2 vs. T1 and T3 vs. T1

A total of 4212 and 5301 DEGs were observed from the 61,241 isoforms, with 1701 up-regulated (UR) and 2511 down-regulated (DR) at T2 vs. T1, and 2544 UR and 2757 DR at T3 vs. T1 (Figure 2), based on the FPKM values (Figure S6), principal component analysis (PCA) (Figure S7) and Pearson correlation analysis (Figure S8). The cluster heat map of the DEGs at T2 vs. T1 and T3 vs. T1 was shown in Figure 3, which provides further analysis such as identification of the gene functions or gene response analysis.

**Figure 2.** Volcano plot of differential expression at T2 vs. T1 (A) and T3 vs. T1 (B).

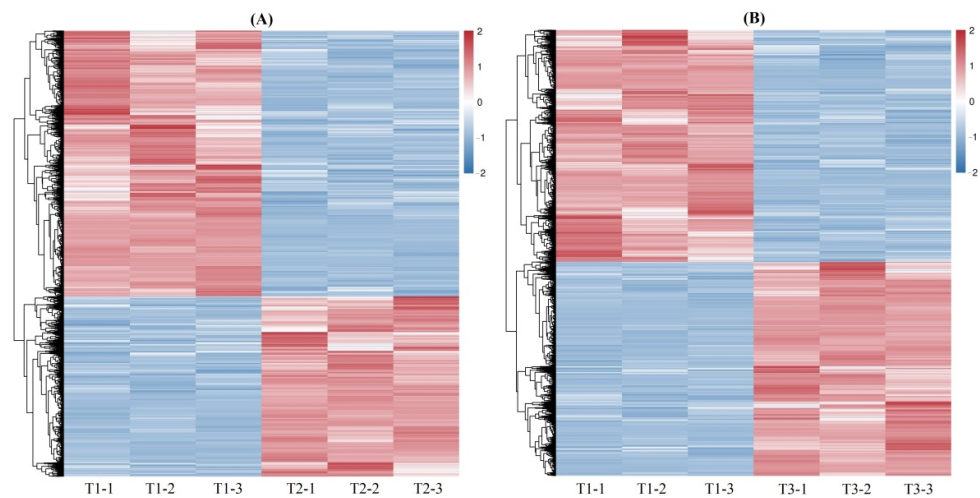


Figure 3. Cluster heat map of the DEGs at T2 vs. T1 (A) and T3 vs. T1 (B).

3.3.2. GO and KEGG Enrichments of DEGs

Based on the GO system, the DEGs were classified into three ontologies including biological process (BP), cellular component (CC) and molecular function (MF) (Figure S9). Based on the KEGG database, at T2 vs. T1, the 4212 DEGs were enriched into 127 pathways, such as plant hormone signal transduction, starch and sucrose metabolism, and phenylpropanoid biosynthesis; at T3 vs. T1, the 5301 DEGs were enriched into 128 pathways, such as biosynthesis of secondary metabolites, the MAPK signaling pathway, and plant and starch and sucrose metabolism (Figure S10).

3.3.3. Uncovering DEGs Involved in Flowering during Vernalization

Based on the regulatory pathways of flowering genes in *Arabidopsis* [30–32], 151 and 155 genes involved in regulating flowering were, respectively, uncovered from the 4212 DEGs at T2 vs. T1 and 5301 DEGs at T3 vs. T1, and 104 co-expressed genes were classified into six categories: FLC expression (22), sucrose metabolism (12), hormone response (18), circadian clock (2), downstream floral integrators and meristem identity (15), and cold response (35) (Figure 4). The 104 DEGs exhibited a -3.68 - to 4.07 -fold and -8.75 - to 9.48 -fold differential expression at T2 vs. T1 and T3 vs. T1, respectively (Figure 5). The sequence details of the isoforms involved in the 104 co-expressed genes are shown in Table S2.

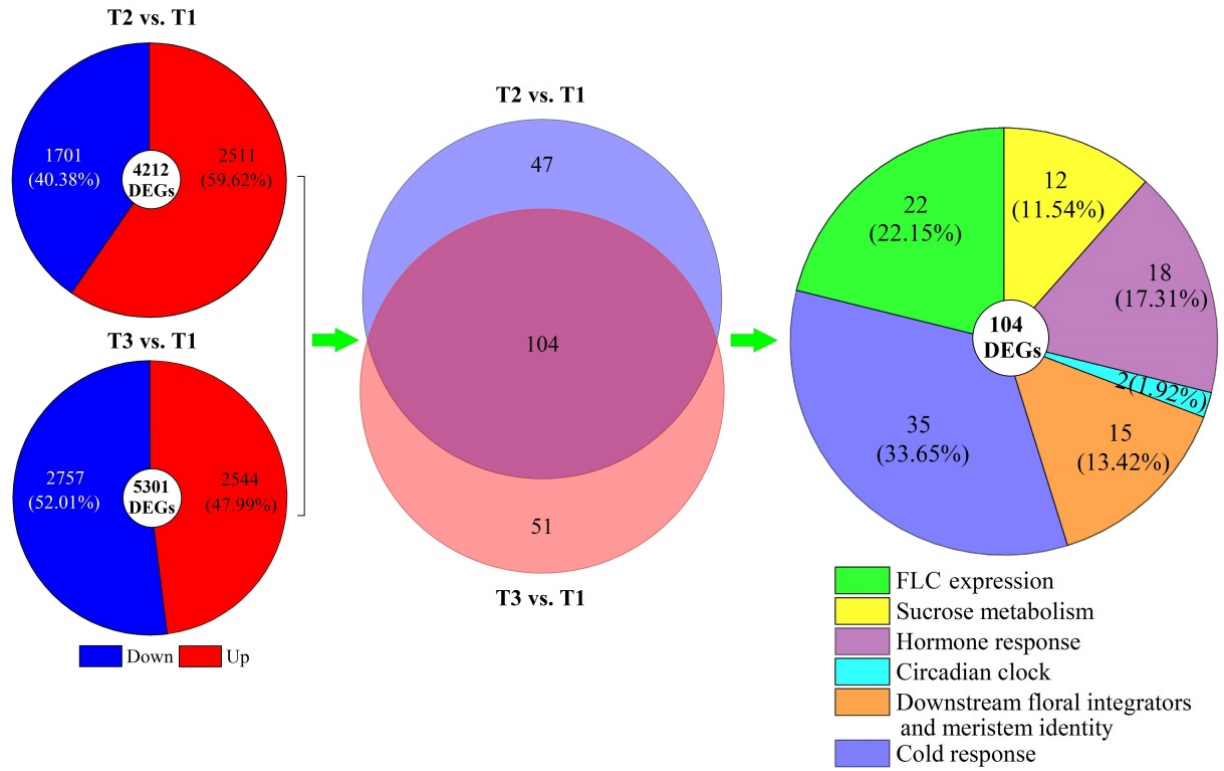


Figure 4. Distribution and classification of DEGs in *A. sinensis* at T2 vs. T1 and T3 vs. T1.

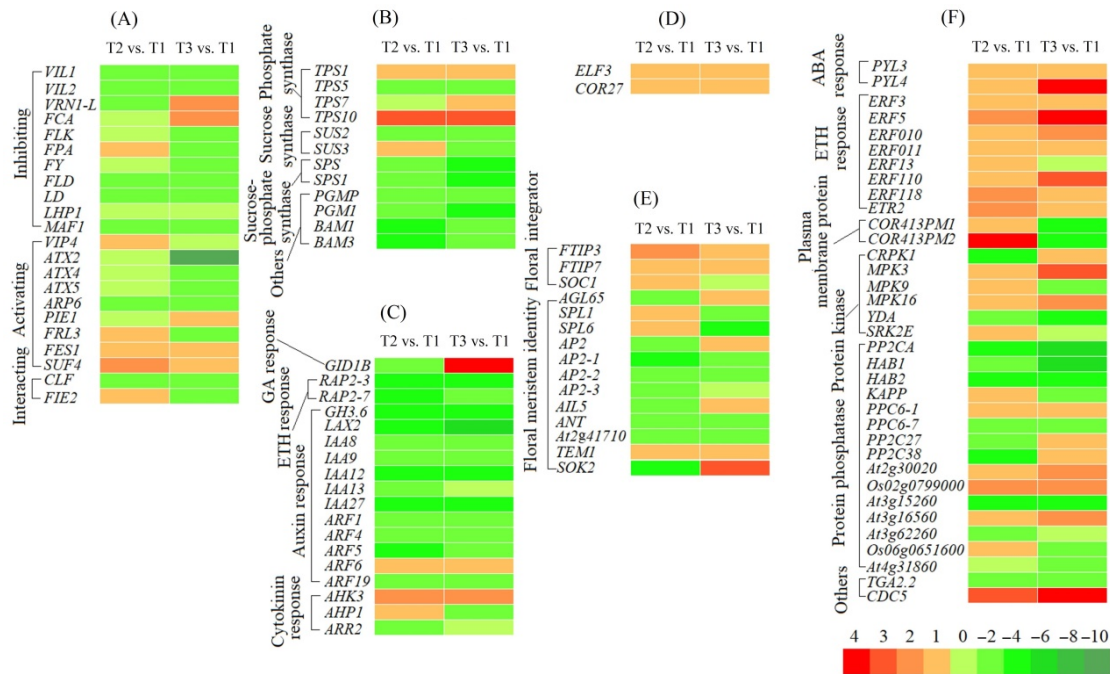


Figure 5. Heat map of the 104 DEGs involved in flowering at T2 vs. T1 and T3 vs. T1. The differential expression level is based on FPKM values; gene abbreviations are provided in Tables S3–S8. The subfigures (A): FLC expression, (B): sucrose metabolism, (C): hormone response, (D): circadian clock, (E): downstream floral integrators and meristem identity, and (F): cold response.

3.3.4. DEGs Involved in FLC Expression

Out of the 104 DEGs involved in regulatory pathways of flowering, 22 genes were involved in FLC expression (Figure 5A, Table S3), with 11 genes inhibiting FLC expression, including vernalization response (*VIL1*, *VIL2* and *VRN1-L*), autonomous pathway [RNA binding (*FCA*, *FLK* and *FPA*); RNA process (*FY*) and chromatin modification (*FLD* and *LD*)], chromo domain protein (*LHP1*) and repressor of RNA polymerase III transcription (*MAF1*); 9 genes activating FLC expression, including PAF1 complex (*VIP4*, *ATX2*, *ATX4* and *ATX5*), SWR1 complex (*ARP6* and *PIE1*) and FRIGIDA-like protein (*FRL3*, *FES1* and *SUF4*); and 2 genes interacting with FLC expression, including polycomb group (PcG) protein (*CLF* and *FIE2*). Fifteen genes were confirmed by qRT-PCR: the RELs of 11 genes inhibiting FLC expression (*VIL1*, *VIL2*, *VRN1-L*, *FCA*, *FLK*, *FPA*, *FY*, *FLD*, *LD*, *LHP1* and *MAF1*) and 4 genes activating FLC expression (*VIP4*, *ATX2*, *ARP6* and *FRL3*) were almost consistent with their FPKM values at T2 vs. T1 and T3 vs. T1 (Figures 5A and 6).

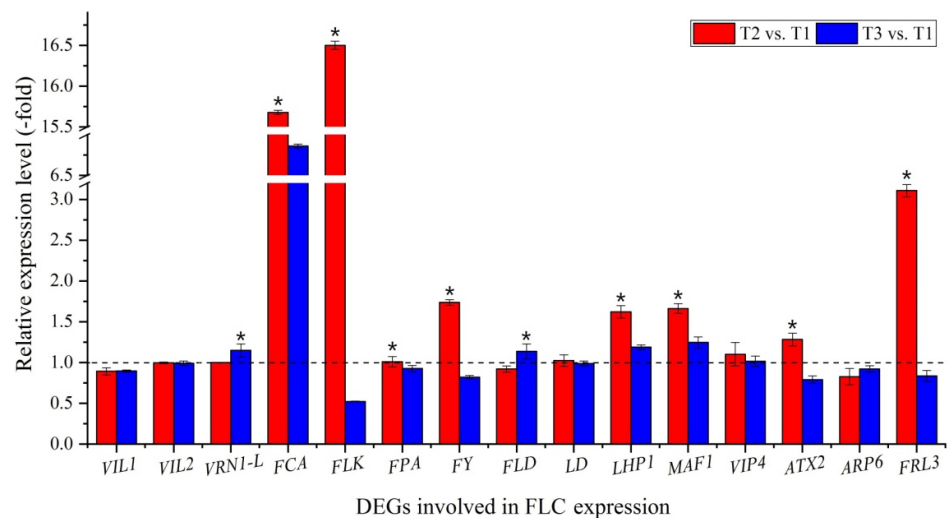


Figure 6. Expression levels of 15 genes involved in FLC expression at T2 vs. T1 and T3 vs. T1. Here and below, “*” represents a significant difference at the $p < 0.05$ level between T2 vs. T1 and T3 vs. T1 for the same gene.

3.3.5. Genes Involved in Sucrose Metabolism

Twelve genes involved in sucrose metabolism were observed to be differentially expressed (Figure 5B, Table S4), with genes encoding trehalose-phosphate synthase (*TPS1*, *TPS5*, *TPS7* and *TPS10*), sucrose synthase (*SUS2* and *SUS3*), sucrose-phosphate synthase (*SPS* and *SPS1*), phosphoglucomutase (*PGMP* and *PGM1*) and beta-amylase (*BAM1* and *BAM3*). Three genes were confirmed using qRT-PCR: the RELs of these three genes (*TPS1*, *SUS3* and *SPS*) were consistent with their FPKM values at T2 vs. T1 and T3 vs. T1 (Figures 5B and 7A). The soluble sugar content exhibited a 0.77-fold decrease at T2 vs. T1 and a 1.13-fold increase at T3 vs. T1 (Figure 7B).

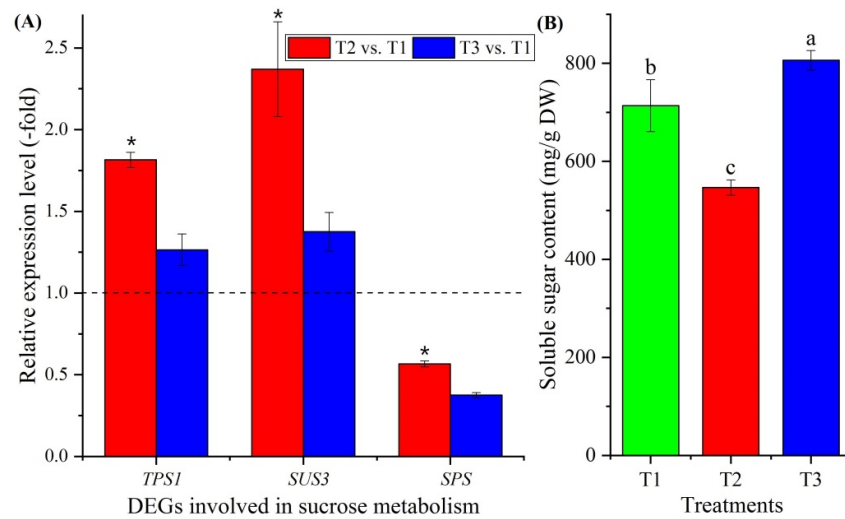


Figure 7. Expression levels of 3 genes involved in sucrose metabolism at T2 vs. T1 and T3 vs. T1 (A), and changes in soluble sugars contents at T1, T2 and T3 (B). Here and below, “*” represents a significant difference at the $p < 0.05$ level between T2 vs. T1 and T3 vs. T1 for the same gene; the use of different letters represents a significant difference ($p < 0.05$) at different temperature treatments.

3.3.6. Genes Involved in Hormone Response

Eighteen genes involved in hormone response were observed to be differentially expressed (Figure 5C, Table S5), with gibberellin (GA) response (*GID1B*), ethylene (ETH) response (*RAP2-3* and *RAP2-7*), indole-3-acetic acid (IAA)-amido synthetase (*GH3.6*), auxin transport (*LAX2*), auxin response (*IAA8*, *IAA9*, *IAA12*, *IAA13*, *IAA27*, *ARF1*, *ARF4*, *ARF5*, *ARF6* and *ARF19*) and cytokinin (CTK) response (*AHK3*, *AHP1* and *ARR2*). Five genes were confirmed by qRT-PCR, and the RELs of these five genes (*GID1B*, *RAP2-7*, *IAA13*, *ARF1* and *AHK3*) were consistent with their FPKM values at T2 vs. T1 and T3 vs. T1 (Figures 5C and 8A). The contents of GA₃ and IAA exhibited a 1.86- and 1.59-fold increase at T2 vs. T1 and a 0.42- and 0.65-fold decrease at T3 vs. T1, respectively (Figure 8B,C).

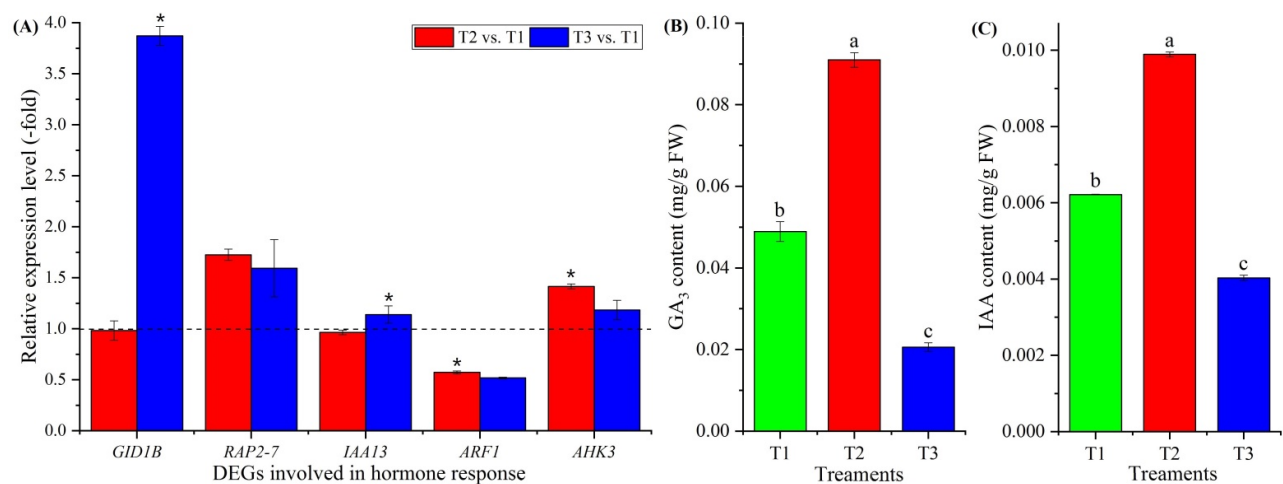


Figure 8. Expression levels of 5 genes involved in hormone response at T2 vs. T1 and T3 vs. T1 (A), and changes in GA₃ and IAA contents at T1, T2 and T3 (B,C). Here and below, “*” represents a significant difference at the $p < 0.05$ level between T2 vs. T1 and T3 vs. T1 for the same gene; the use of different letters represents a significant difference ($p < 0.05$) at different temperature treatments.

3.3.7. DEGs Involved in Circadian Clock

Two genes involved in circadian clock were observed to be differentially expressed (Figure 5D, Table S6), including a transcription factor part of a circadian clock (*ELF3*) and cold-regulated protein (*COR27*). These two genes were confirmed using qRT-PCR, and the RELs were consistent with their FPKM values at T2 vs. T1 and T3 vs. T1 (Figures 5D and 9A).

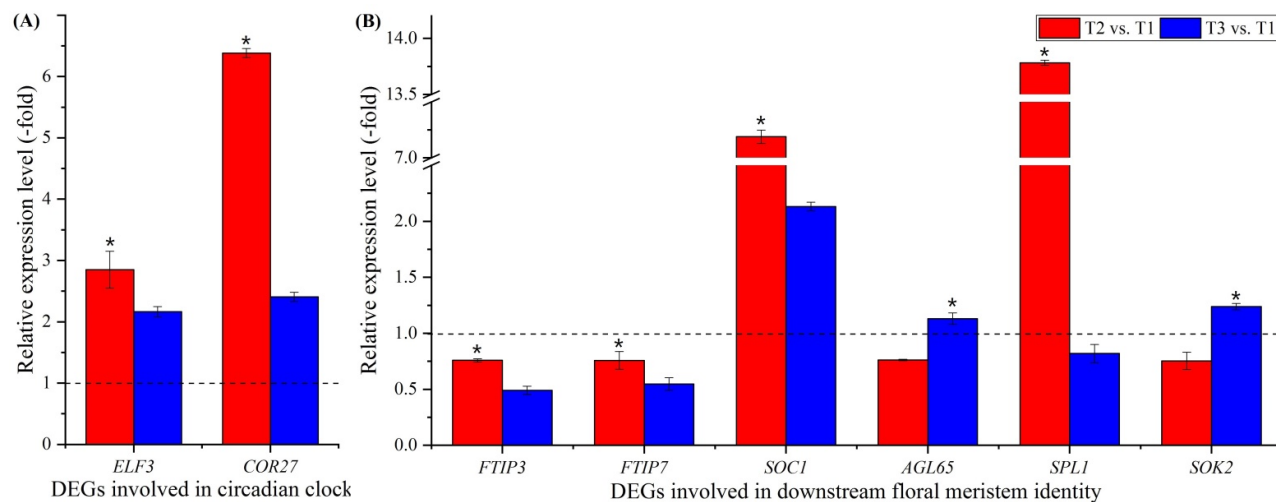


Figure 9. Expression levels of 2 genes involved in the circadian clock (A), and 6 genes involved in downstream floral meristem identity at T2 vs. T1 and T3 vs. T1 (B). Here and below, “*” represents a significant difference at the $p < 0.05$ level between T2 vs. T1 and T3 vs. T1 for the same gene; the use of different letters represents a significant difference ($p < 0.05$) at different temperature treatments.

3.3.8. DEGs Involved in Downstream Floral Integrators and Meristem Identity

Fifteen genes involved in downstream floral integrators and meristem identity were observed to be differentially expressed (Figure 5E, Table S7); these included floral integrators (*FTIP3*, *FTIP7* and *SOC1*) and floral meristem identity (*AGL65*, *SPL1*, *SPL6*, *AP2*, *AP2-1*, *AP2-2*, *AP2-3*, *AIL5*, *ANT*, *At2g41710*, *TEM1* and *SOK2*). Six genes were confirmed by qRT-PCR, and the RELs of six of these genes (*FTIP3*, *FTIP7*, *SOC1*, *AGL65*, *SPL1* and *SOK2*) were consistent with their FPKM values at T2 vs. T1 and T3 vs. T1 (Figures 5E and 9B).

3.3.9. DEGs Involved in Cold Response

Thirty-five genes involved in cold-stress response were observed to be differentially expressed (Figure 5F, Table S8), with abscisic acid (ABA) response (*PYL3* and *PYL4*), ETH response (*ERF3*, *ERF5*, *ERF010*, *ERF011*, *ERF13*, *ERF110*, *ERF118* and *ETR2*), cold-regulated plasma membrane proteins (*COR413PM1* and *COR413PM2*), cold-responsive protein kinase (*CRPK1*, *MPK3*, *MPK9*, *MPK16*, *YDA* and *SRK2E*), protein phosphatase (*PP2CA*, *HAB1*, *HAB2*, *KAPP*, *PPC6-1*, *PPC6-7*, *PP2C27*, *PP2C38*, *At2g30020*, *Os02g0799000*, *At3g15260*, *At3g16560*, *At3g62260*, *Os06g0651600* and *At4g31860*), and other stress-response factors and protein (*TGA2.2* and *CDC5*). Nine genes were confirmed by qRT-PCR, and the RELs of these nine genes (*PYL3*, *ERF110*, *ETR2*, *COR413PM1*, *CRPK1*, *MPK3*, *SRK2E*, *PP2CA* and *HAB1*) were almost consistent with their FPKM values at T2 vs. T1 and T3 vs. T1 (Figures 5F and 10A). The ABA content exhibited a 0.49- and 0.84-fold decrease at T2 vs. T1 and T3 vs. T1, respectively (Figure 10B).

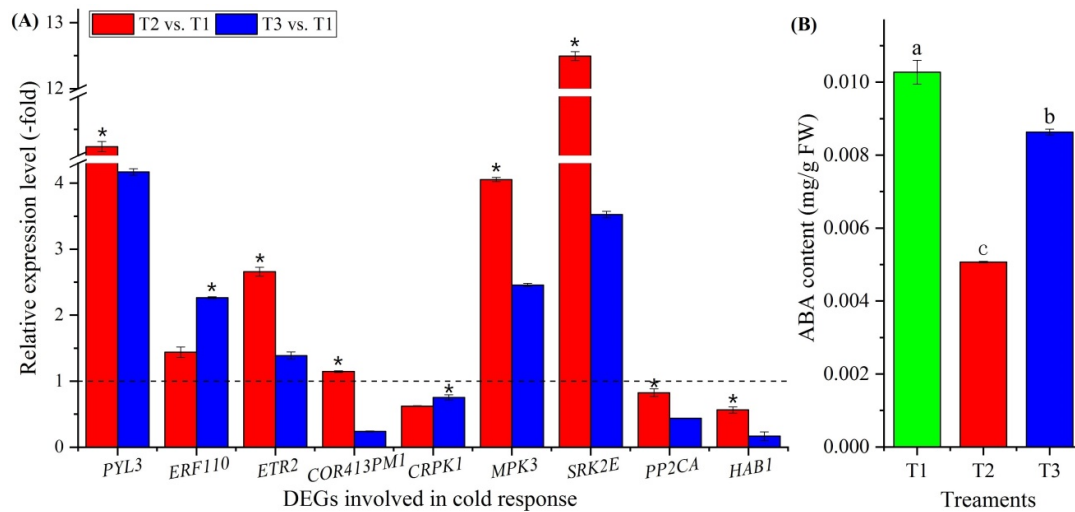


Figure 10. Expression levels of 9 genes involved in cold response (A) and changes in ABA contents at T1, T2 and T3 (B). Here and below, “*” represents a significant difference at the $p < 0.05$ level between T2 vs. T1 and T3 vs. T1 for the same gene; the use of different letters represents a significant difference ($p < 0.05$) at different temperature treatments.

4. Discussion

Vernalization is the process whereby flowering is promoted by prolonged exposure to a cold treatment given to a fully hydrated seed or a growing plant; without vernalization, plants show delayed flowering or remain vegetative. Meanwhile, vernalization can be lost at high temperatures and avoided below freezing temperatures [33]. Extensive studies have reported that vernalization suppresses the expression of genes encoding the repressors of flowering [34]; moreover, the gene network of flowering time has been mapped with known genetic and epigenetic regulators in the model plant *Arabidopsis thaliana* [31,32]. For *A. sinensis*, the effective temperature range for vernalization is from 0 to 5 °C with a duration 57 to 85 d, and the vernalization can be effectively avoided with exposure of seedlings to temperatures from −2 to −12 °C [10–13]. However, gene-regulatory networks involved in the flowering of *A. sinensis* during the vernalization have not been revealed. By storing seedlings at 0 °C for 14 d (uncompleted vernalization, T1) and 60 d (completed vernalization, T2), as well as at −3 °C for 125 d (avoided vernalization, T3), a total of 4212 and 5301 genes were differentially expressed, and 151 and 155 genes were involved in flowering at T2 vs. T1 and T3 vs. T1, respectively. Based on their biological functions, 104 co-expressed genes were classified into 6 categories: FLC expression, sucrose metabolism, hormone response, circadian clock, downstream floral integrators and meristem identity, and cold response.

4.1. Genes Involved in FLC Expression

FLC is a MADS-box transcriptional regulator that acts as a potent repressor of flowering [35]. Several genes inhibit FLC expression; among these, 11 genes encoding proteins are involved in vernalization response, including VIN3-like proteins (VIL1 and VIL2) that inhibit the expression of FLC and FLM, which are associated with an epigenetically silenced state and with acquisition of competence to flower [36–39], and VRN1-like (VRN1-L), which may act as transcriptional repressor of FLC [40]. The genes that inhibit FLC expression also include the genes involved in the autonomous pathway, including proteins that control flowering time, FCA and FPA, which decrease FLC expression and act redundantly with each other to prevent the expression of distally polyadenylated antisense RNAs at the FLC locus [41–43]; flowering locus K (FLK), which represses FLC expression and post-transcriptional modification [44,45]; another protein controlling flowering time, FY, which decreases FLC expression and is required for the

negative autoregulation of FCA expression [46,47]; and FLOWERING LOCUS D (FLD) and LUMINIDEPENDENS (LD), which decrease FLC expression via chromatin modification [48–50]. Finally, there are two other genes that inhibit FLC expression: chromo domain protein LHP1 (LHP1), which is a structural component of heterochromatin involved in gene repression via methylating H3-K9 [51], and MAF1 homolog (MAF1), which is an element of the TORC10 signaling pathway and represses RNA polymerase III transcription [52].

For genes activating FLC expression, there are nine genes encoding proteins involved in the PAF1 complex: LEO1 homolog (VIP4), which is involved in histone modifications and is required for the FLC expression [53,54]; histone-lysine N-methyltransferases (ATX2, ATX4 and ATX5), which dimethylate H3K4me2 and are involved in epigenetic regulation of FLC and FT [55–57]; genes involved in the SWR1 complex, namely actin-related protein 6 (ARP6) and PHOTOPERIOD-INDEPENDENT EARLY FLOWERING 1 (PIE1), which are associated with transcriptional regulation of selected genes (e.g., *FLC*) via chromatin remodeling; ARP6, which is required for the activation of *FLC* and *FLC/MAF* genes expression through both histone H3 and H4 acetylation and methylation [58,59]; PIE1, which is required for the reactivation of *FLC* [60,61]. There are also genes involved in the FRIGIDA-like protein: FRIGIDA-like protein 3 (FRL3), which trimethylates H3K4, increasing *FLC* expression [62]; FRIGIDA-ESSENTIAL 1 (FES1), which acts cooperatively with *FRI* or *FRL1* to promote *FLC* expression [63,64]; and SUPPRESSOR OF FRI 4 (SUF4), which recruits the FRI-C complex to the FLC promoter and is required for FRI-mediated FLC activation and maintains high levels of *FLC* expression [63,65].

There are also genes interacting with FLC expression: these include two genes involved in PcG protein: histone-lysine N-methyltransferase CLF (CLF) and PcG protein FIE1 (FIE2), which are required to maintain the transcriptionally repressive state of homeotic genes by methylating H3-K27, rendering chromatin heritably changed in its expressibility [66,67]. According to the RELs of genes calculated with the FPKM value and validated using qRT-PCR, the genes involved in inhibiting *FLC* expression were up-regulated, while the genes involved in activating *FLC* expression were down-regulated at T2 vs. T1 (during vernalization); however, these genes showed the opposite expression levels at T3 vs. T1 (freezing temperature avoided vernalization) (Figure 6; Table S3). These findings are consistent with previous studies with higher flowering rates at T2 with lower flowering rates at T3 compared with T1 (Figure S2).

4.2. Genes Involved in Sucrose Metabolism

For vernalization to occur, sources of energy (sugars) and carbohydrate metabolism are required [33,68]. Twelve genes were found to be involved in sucrose metabolism: trehalose-phosphate synthases (TPS1, TPS5, TPS7 and TPS10), which are required for vegetative growth and transition to flowering by regulating starch and sucrose degradation [69–71]; sucrose synthases (SUS2 and SUS3), which provide UDP glucose and fructose for various metabolic pathways [72]; sucrose-phosphate synthases (SPS and SPS1), which regulate sucrose synthesis from UDP glucose and fructose-6-phosphate [73]; phosphoglucosyltransferases (PGMP and PGM1), which participate in both the breakdown and the synthesis of glucose [74]; and beta-amylases (BAM1 and BAM3), which play roles in circadian-regulated starch degradation and maltose metabolism [75]. According to the RELs, the genes involved in sucrose and starch degradation were up-regulated during vernalization (T2) and down-regulated at freezing temperature (T3) compared with T1, while the genes involved in sucrose and starch biosynthesis showed the opposite expression levels (Figure 7A; Table S4). This differential expression of genes is consistent with the change in soluble sugar contents at T1, T2 and T3 (Figure 7B).

4.3. Genes Involved in Hormone Response

The GA pathway is required for early flowering by promoting the expression of the *LFY* gene; meanwhile, other growth hormones (e.g., ETH, IAA and CTK) can either inhibit or promote flowering [33]. Here, there were 18 genes that were found to be involved in the hormone response, including the GA receptor *GID1B* (*GID1B*), which functions as soluble GA receptor interacting with specific DELLA proteins, known as repressors of GA-induced growth and flower development [76]; ETH-responsive transcription factors (*RAP2-3* and *RAP2-7*), which negatively regulate the transition to flowering time and cause a delay in flowering time [77]; IAA-amido synthetase (*GH3.6*), which is involved in auxin signal transduction [78]; auxin transporter-like protein 2 (*LAX2*), which is involved in proton-driven auxin influx and basipetal auxin transport [79,80]; Aux/IAA proteins (*IAA8*, *IAA9*, *IAA12*, *IAA13* and *IAA27*), which function as repressors of early auxin response genes at low auxin concentrations by forming heterodimers with auxin response factors (ARFs) [81]; ARFs (*ARF1*, *ARF4*, *ARF5*, *ARF6* and *ARF19*), which act as transcriptional repressors (e.g., *IAA2*, *IAA3* and *IAA7*) by forming heterodimers with Aux/IAA proteins and promoting flowering [82,83]; and CTK response, i.e., histidine kinase 3 (*AHK3*), which the cytokinin-dependent flower-development-regulation pathway requires [84]; histidine-containing phosphotransfer protein 1 (*AHP1*), which functions as a two-component phosphorelay mediator between cytokinin sensor histidine kinases and response regulators (B-type ARR) [85]; and two-component response regulator *ARR2* (*ARR2*), which functions as a response regulator involved in the His-to-Asp phosphorelay signal transduction system [86]. Based on the RELs, the genes involved in promoting flowering were up-regulated during vernalization but down-regulated at freezing temperatures (Figure 8A; Table S5). Meanwhile, the change in GA₃ and IAA contents was also shown to be higher at vernalization compared with freezing temperatures (Figure 8B,C).

4.4. Genes Involved in the Circadian Clock

Flowering is often triggered when plants are exposed to appropriate day lengths, which requires the circadian clock to measure the passage of time [87]. Recent studies have found that the circadian clock is also controlled by temperatures [88]. Here, two genes were found to be involved in the circadian clock: *EARLY FLOWERING 3* (*ELF3*), which is a transcription factor part of a circadian-clock input pathway and can regulate the initiation of flowering [89,90], and cold-regulated protein (*COR27*), which is a negative regulator of freezing tolerance that, together with *COR28*, is involved in central circadian clock regulation and in flowering promotion by binding to the chromatin of clock-associated evening genes (e.g., *ELF4*) [91,92]. According to the RELs, the genes (*ELF3* and *COR27*) favoring the initiation of flowering were up-regulated (Figure 9A; Table S6), which accelerates the formation of leaves and eventually the physiological age during vernalization [33].

4.5. Genes Involved in the Downstream Floral Integrators and Meristem Identity

Flower formation occurs at the SAM and is a complex morphological event that is regulated by several genes [33]. Here, 15 genes were found to be involved in downstream floral integrators and meristem identity. Three of these genes were involved in floral integrators: FT-interacting protein 3 (*FTIP3*), which is required for the proliferation and differentiation of shoot stem cells in SAM [93]; FT-interacting protein 7 (*FTIP7*), which promotes nuclear translocation of the transcription factor homeobox 1, directly suppressing the auxin biosynthetic gene *YUCCA4* [94]; and *SOC1*, which integrates signals from the photoperiod, vernalization and autonomous floral induction pathways [95].

Ten genes are involved in the floral meristem identity: agamous-like MADS-box protein *AGL65* (*AGL65*), which forms a heterodimer with the MADS-box protein *AGL104* [96]; squamosa promoter-binding-like proteins (*SPL1* and *SPL6*), which bind

specifically to the consensus nucleotide sequence of the AP1 promoter [97]; APETALA 2 and -like proteins (AP2, AP2-1, AP2-2, AP2-3, AIL5, ANT and At2g41710), which are involved in initiation and development of organs, including floral organs [98–101]; AP2/ERF and B3 domain-containing transcription repressor TEM1 (TEM1), which is a transcriptional repressor of flowering time in plants that prefer long days and acts directly upon FT expression [102]; and *SOK2*, which can influence cell division orientation to coordinate cell polarization, which is fundamental for tissue morphogenesis in multicellular organisms [103–105]. According to the RELs, the genes involved in floral integrators and meristem identity were up-regulated during vernalization but down-regulated at freezing temperatures (Figure 9B; Table S7). These findings further indicate that vernalization enhances the early flowering of *A. sinensis*.

4.6. Genes Involved in the Cold Response

Vernalization cannot be completed in the context of short exposures to cold, which might occur during cases of fluctuating temperatures, after which plants may face and adapt to low temperatures [34]. Here, 35 genes were found to be involved in the cold response, including 2 genes involved in ABA response: ABA receptors PYL3 and PYL4 (PYL3 and PYL4), which act as positive regulators of tolerance to cold stress [106]. Genes involved in the cold response also include those involved in the ETH response: ethylene-responsive transcription factors (ERF3, ERF5, ERF010, ERF011, ERF13, ERF110 and ERF118), which regulate gene expression by stress factors and by components of stress signal transduction pathways [107,108], and ETH receptor 2 (ETR2), which acts as a redundant negative regulator of ETH signaling [109]. They also include two genes involved in cold-regulated plasma membrane proteins: cold-regulated 413 plasma membrane proteins (COR413PM1 and COR413PM2), which are up- and down-regulated, respectively, in response to low temperatures [110]. In addition, they include six genes involved in cold-responsive protein kinase: cold-responsive protein kinase 1 (CRPK1), which is a negative regulator of freezing tolerance [111]; mitogen-activated protein kinases (MPK3, MPK9, MPK16 and YDA), which are associated with the ABA-activated signaling pathway in response to oxidative stress and freezing [112,113]; serine/threonine-protein kinase SRK2E (SRK2E), which is an activator of the ABA signaling pathway [114]. They also included 15 genes that were found to be involved in protein phosphatases (PP2CA, HAB1, HAB2, KAPP, PPC6-1, PPC6-7, PP2C27, PP2C38, At2g30020, Os02g0799000, At3g15260, At3g16560, At3g62260, Os06g0651600 and At4g31860), which regulate numerous ABA responses such as cold stress [115–117]. In addition, transcription factor TGA2.2 (TGA2.2) is involved in the defense response [118], and cell division cycle 5-like protein (CDC5) is involved in mRNA splicing and cell cycle control and may also play a role in the response to DNA damage [119,120]. According to the RELs, most of the genes involved in cold stress were up-regulated (Figure 10A; Table S8), and the ABA contents increased in response to vernalization and freezing temperatures (Figure 10B), which trigger the stress response for the seedlings adapting to low temperatures.

4.7. Proposed Regulatory Networks of Flowering Genes in *A. sinensis* during Vernalization

Based on the functional analysis and the regulatory pathways of flowering genes in the model plant *Arabidopsis* [30–32], a schematic representation of the proposed regulatory networks of flowering genes in *A. sinensis* during vernalization was created and is shown in Figure 11. Briefly, during the vernalization, four pathways that regulate flowering time were observed: the vernalization pathway, the autonomic pathway, the age pathway and the GA (hormone) pathway. In the vernalization pathway, the expression of *FLC* is inhibited by the genes *VIL1*, *VIL2*, *VRN1-L*, *LHP1* and *MAF1* but activated by the genes encoding the PAF1 complex (e.g., *VIP4*, *ATX2* and *ATX*), the SWR1 complex (*ARR6* and *PIE1*) and FRIGIDA-like proteins (*FRL3*, *FES* and *SUF4*) and regulated by proteins of the polycomb group (*CLF* and *FIE2*). In the autonomic pathway, the expression of *FLC* is inhibited by the genes involved in RNA binding (*FCA*, *FPA* and *FLK*), the

RNA process (*FY*) and chromatin modification (*FLD* and *LD*). In the age pathway, the expression of *SOC1* is promoted by the genes encoding SPLs (*SPL1* and *SPL6*), which can be positively regulated by the genes involved in sucrose metabolism (e.g., *TPS1*, *SUS2* and *SPS*). In the GA (hormone) pathway, the expression of *SOC1* is promoted by the genes involved in the CTK response (*AHK3*, *AHP1* and *ARR2*) but inhibited by the genes involved in ETH response (*RAP2-3* and *RAP2-7*) and IAA (e.g., *GH3.6*, *LAX2* and *IAA8*); the expression of *AP1* is promoted by the DELLA protein, which is inhibited by the genes involved in the GA response (*GID1B*). Additionally, the expression of *FT* (*FTIP3* and *FTIP7*) is promoted by the genes involved in the circadian clock (*ELF3* and *COR27*), as well as AP2 and -like proteins (e.g., *AP2*, *AP2-1* and *AIL5*), but inhibited by the gene *TEM1*. The expression of *SOC1* is also promoted by the gene *AGL65*. The coordinated expression of these genes during vernalization confers the transition of seedlings from vegetative growth to flowering of *A. sinensis*.

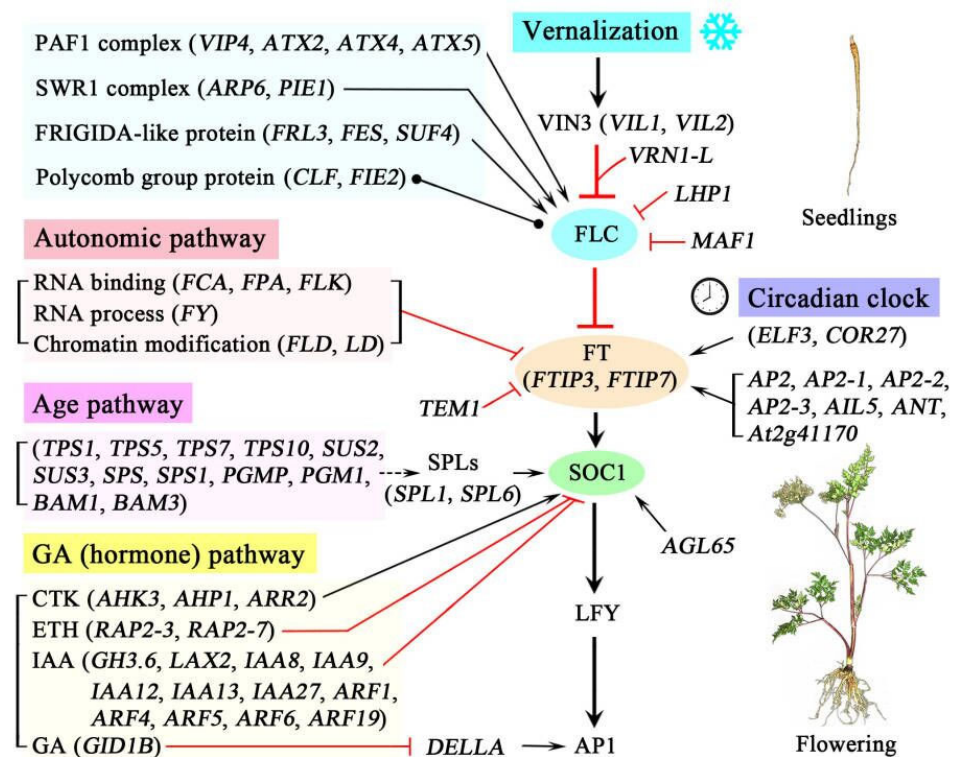


Figure 11. Schematic representation of the proposed regulatory networks of flowering genes in *A. sinensis* during vernalization. The arrows indicate a promotion, with T-ends with red color indicating an inhibition, round dots at both ends mark an interaction without a known direction, and dashed lines indicate an indirect interaction.

5. Conclusions

The DEGs observed in *A. sinensis* during vernalization strongly suggest that transcription-based regulation occurs for the transition of seedlings from vegetative growth to flowering. The expression level of genes involved in flowering and the cold response during vernalization were almost consistent with changes in sugars and hormone contents. There are four pathways of genes that are required for regulating flowering, including the vernalization pathway, the autonomic pathway, the age pathway and the GA (hormone) pathway. While genes involved in flowering during vernalization have been mapped here, additional studies are required to determine the causative role of these genes in promoting or inhibiting the expression of the central genes (e.g., *VINs*, *SOC1* and *FT*).

Supplementary Materials: The following supporting information can be downloaded at: <https://www.mdpi.com/article/10.3390/plants11101355/s1>, Supplemental figure legends: Figure S1. Morphological characteristics of *A. sinensis* seedlings; Figure S2. Flowering rate of *A. sinensis* after the seedlings stored at T1, T2 and T3; Figure S3. The cycle threshold (Ct) values of *ACT* gene at different volumes (0.25, 0.5, 1.0, 1.5, 2.0 and 3.0 μ L) via PCR amplification with three replications; Figure S4. The standard curve of the *ACT* gene; Figure S5. The number and length distribution of high-fidelity reads (A), polished high-quality isoforms (B) and full-length isoforms (C); Figure S6. Violin plot of expressions in T1, T2 and T3; Figure S7. PCA analysis of T1, T2 and T3; Figure S8. Pearson correlation analysis between T1, T2 and T3; Figure S9. Gene Ontology (GO) enrichment of DEGs at T2 vs. T1 and T3 vs. T1; Figure S10. KEGG enrichment of DEGs at T2 vs. T1 and T3 vs. T1. Supplemental table legends: Table S1. Sequences of primers employed in qRT-PCR analysis; Table S2. The sequence details of the isoforms involved in the 104 co-expressed genes at T2 vs. T1 and T3 vs. T1; Table S3. DEGs involved in FLC expression at T2 vs. T1 and T3 vs. T1; Table S4. DEGs involved in sucrose metabolism at T2 vs. T1 and T3 vs. T1; Table S5. DEGs involved in hormone response at T2 vs. T1 and T3 vs. T1; Table S6. DEGs involved in the circadian clock at T2 vs. T1 and T3 vs. T1; Table S7. DEGs involved in the downstream floral integrators and meristem identity at T2 vs. T1 and T3 vs. T1; Table S8. DEGs genes involved in cold response at T2 vs. T1 and T3 vs. T1.

Author Contributions: M.L. (Mimi Luo): Data curation, Investigation, Writing—Original Draft; X.L.: Data Curation, Investigation, Writing—Original Draft; H.S.: Methodology, Investigation; M.L. (Meiling Li): Formal analysis; M.L. (Mengfei Li): Conceptualization, Project administration, Supervision, Writing—Review and Editing; J.W.: Conceptualization, Funding Acquisition, Resources. All authors have read and agreed to the published version of the manuscript.

Funding: This research was funded by the State Key Laboratory of Aridland Crop Science/Gansu Agricultural University (GSCS-2021-Z03), National Natural Science Foundation of China (32160083), China Agriculture Research System of MOF and MARA (CARS-21), and the Assurance Project of Ecological Planting and Quality of Daodi Herbs (202103003).

Institutional Review Board Statement: Not applicable.

Informed Consent Statement: Not applicable.

Data Availability Statement: The datasets are available at NCBI, with BioSample accession SAMN24046640 to SAMN24046648; SRA accession SRR17235563 to SRR17235571 (9 objects) with every treatment three replicates; and the BioProject's metadata are available at <https://www.ncbi.nlm.nih.gov/bioproject/PRJNA789039>, accessed on 14 December 2021.

Conflicts of Interest: The authors declare no conflict of interest.

Abbreviations

AGL65, agamous-like MADS-box protein AGL65; COR27, cold-regulated protein 27; DEGs, differentially expressed genes; ELF3, protein EARLY FLOWERING 3; ERF, ethylene-responsive transcription factor; FCA, flowering time control protein FCA; FLC, FLOWERING LOCUS C; FPKM, fragments per kilobase of exon model per million mapped reads; FY, flowering time control protein; GID1B, gibberellin receptor GID1B; IAA, auxin-responsive protein IAA13; KEGG, Kyoto Encyclopedia of Genes and Genomes; KOG, Eukaryotic Orthologous Groups of proteins; Nr, NCBI non-redundant protein; PYL, abscisic acid receptor PYL; RAP2, ethylene-responsive transcription factor RAP2; SAM, shoot apical meristem; SOC1, SUPPRESSOR OF OVEREXPRESSION OF CONSTANS 1; SPL, squamosa promoter-binding-like protein; SPS, sucrose-phosphate synthases; SUS3, sucrose synthase 3; TPS, alpha, alpha-trehalose-phosphate synthase; VIL, VIN3-like protein.

References

1. Zhang, H.Y.; Bi, W.G.; Yu, Y.; Liao, W.B. *Angelica sinensis* (Oliv.) Diels in China: Distribution, cultivation, utilization and variation. *Genet. Resour. Crop Evol.* **2012**, *59*, 607–613.
2. Hook, I.L.I. Danggui to *Angelica sinensis* root: Are potential benefits to European women lost in translation a review. *J. Ethnopharmacol.* **2014**, *152*, 1–13.
3. Committee for the Pharmacopoeia of PR China. *Pharmacopoeia of the People's Republic of China*; China Medical Science and Technology Press: Beijing, China, 2015; p. 133.
4. Ma, J.P.; Guo, Z.B.; Jin, L.; Li, Y.D. Phytochemical progress made in investigations of *Angelica sinensis* (Oliv.) Diels. *Chin. J. Nat. Med.* **2015**, *13*, 241–249.

5. Upton, R. *American Herbal Pharmacopoeia and Therapeutic Compendium: Dang Gui Root-Angelica sinensis (Oliv.)*; American Herbal Pharmacopoeia: Scotts Valley, CA, USA, 2003; pp. 1–41.
6. Wei, W.L.; Zeng, R.; Gu, C.M.; Qu, Y.; Huang, L.F. *Angelica sinensis* in China-A review of botanical profile, ethnopharmacology, phytochemistry and chemical analysis. *J. Ethnopharmacol.* **2016**, *190*, 116–141.
7. Huang, L.Q.; Jin, L. *Suitable Technology for Production and Processing of Angelica sinensis*; China Pharmaceutical Science and Technology Press: Beijing, China, 2018; pp. 1–14.
8. Li, Y.D. *Research on Angelica sinensis (Oliv.) Diels*; Science Press: Beijing, China, 2021; pp. 36–45.
9. Li, M.L.; Cui, X.W.; Jin, L.; Li, M.F.; Wei, J.H. Bolting reduces ferulic acid and flavonoid biosynthesis and induces root lignification in *Angelica sinensis*. *Plant Physiol. Biochem.* **2022**, *170*, 171–179.
10. Wang, W.J. Analysis and control of early bolting characteristic of *Angelica sinensis*. *J. Northwest Univ. (Nat. Sci. Ed.)* **1977**, *7*, 32–39.
11. Jia, Z.; Di, S.Q.; Zhao, F.Y.; Li, S.X.; Wang, S.C. Effects of different low overwintering temperatures on *Angelica* vernalization and premature bolting. *Agric. Sci. Technol.* **2018**, *19*, 55–62.
12. Li, M.F.; Kang, T.L.; Jin, L.; Wei, J.H. Research progress on bolting and flowering of *Angelica sinensis* and regulation pathways. *Chin. Tradit. Herbal Drugs* **2020**, *51*, 5894–5899.
13. Wang, W.J. Technology and principle of seedling frozen storage of *Angelica sinensis*. *J. Chin. Med. Mat.* **1979**, *3*, 1–5.
14. Yao, L. Effect of shading during the nursery of *Angelica sinensis* on bolting rate and economic characters. *Gansu Agric. Sci. Technol.* **2005**, *10*, 54–55.
15. Li, J.; Li, M.L.; Zhu, T.T.; Zhang, X.N.; Li, M.F.; Wei, J.H. Integrated transcriptomics and metabolites at different growth stages reveals the regulation mechanism of bolting and flowering of *Angelica sinensis*. *Plant Biol.* **2021**, *23*, 574–582.
16. Li, M.F.; Li, J.; Wei, J.H.; Paré, P.W. Transcription controls for early bolting and flowering in *Angelica sinensis*. *Plants* **2021**, *10*, 1931.
17. Yu, G.; Zhou, Y.; Yu, J.J.; Hu, X.Q.; Tang, Y.; Yan, H.; Duan, J.A. Transcriptome and digital gene expression analysis unravels the novel mechanism of early flowering in *Angelica sinensis*. *Sci. Rep.* **2019**, *9*, 1–11.
18. Gao, X.; Guo, F.; Chen, Y.; Bai, G.; Liu, Y.X.; Jin, J.Q.; Wang, Q. Full-length transcriptome analysis provides new insights into the early bolting occurrence in medicinal *Angelica sinensis*. *Sci. Rep.* **2021**, *11*, 1–12.
19. Chen, H.G.; Du, T.; Zhu, T.T.; Gao, S.F.; Chai, L.; He, W.W. Study on physiological mechanisms in frozen storage to reduce early bolting of *Angelica sinensis*. *Mod. Tradit. Chin. Med. Mater. Med.-World Sci. Technol.* **2014**, *16*, 203–206.
20. Zhang, E.H.; Huang, P. Effects of vernalization treatment on physiological character of *Angelica sinensis* seedlings. *J. Gansu Agric. Univ.* **1998**, *33*, 240–243.
21. Gordon, S.P.; Tseng, E.; Salamov, A.; Zhang, J.; Meng, X.; Zhao, Z.; Kang, D.; Underwood, J.; Grigoriev, I.V.; Figueroa, M.; et al. Widespread polycistronic transcripts in fungi revealed by single-molecule mRNA sequencing. *PLoS ONE* **2015**, *10*, e0132628.
22. Grabherr, M.G.; Haas, B.J.; Yassour, M.; Levin, J.Z.; Thompson, D.A.; Amit, I.; Adiconis, X.; Fan, L.; Raychowdhury, R.; Zeng, Q.D.; et al. Full-length transcriptome assembly from RNA-Seq data without a reference genome. *Nat. Biotechnol.* **2011**, *29*, 644–652.
23. Chen, S.; Zhou, Y.; Chen, Y.; Gu, J. fastp: An ultra-fast all-in-one FASTQ preprocessor. *Bioinformatics* **2018**, *34*, i884–i890.
24. Kim, D.; Langmead, B.; Salzberg, S.L. HISAT: A fast spliced aligner with low memory requirements. *Nat. Methods* **2015**, *12*, 357–360.
25. Love, M.I.; Huber, W.; Anders, S. Moderated estimation of fold change and dispersion for RNAseq data with DESeq2. *Genome Biol.* **2014**, *15*, 550.
26. Xu, R.; Xu, J.; Li, Y.C.; Dai, Y.T.; Zhang, S.P.; Wang, G.; Liu, Z.G.; Dong, L.L.; Chen, S.L. Integrated chemical and transcriptomic analyses unveils synthetic characteristics of different medicinal root parts of *Angelica sinensis*. *Chin. Herb. Med.* **2020**, *12*, 19–28.
27. Willems, E.; Leyns, L.; Vandesompele, J. Standardization of real-time PCR gene expression data from independent biological replicates. *Anal. Biochem.* **2008**, *379*, 127–129.
28. Dubois, M.; Gilles, K.A.; Hamilton, J.K.; Rebers, P.A.; Smith, F. Colorimetric method for determination of sugars and related substances. *Anal. Chem.* **1956**, *28*, 350–356.
29. Pan, X.Q.; Welti, R.; Wang, X.M. Quantitative analysis of major plant hormones in crude plant extracts by high-performance liquid chromatography-mass spectrometry. *Nat. Protoc.* **2010**, *5*, 986–992.
30. Banta, J.A.; Purugganan, M.D. The genetics and evolution of flowering time variation in plants: Identifying genes that control a key life history transition. In *Mechanisms of Life History Evolution*; Flatt, T., Heyland, A., Eds.; Oxford University Press Inc.: New York, NY, USA, 2011; pp. 114–126.
31. Blümel, M.; Dally, N.; Jung, C. Flowering time regulation in crops-what did we learn from *Arabidopsis*? *Curr. Opin. Biotechnol.* **2015**, *32*, 121–129.
32. Yang, X.F.; Li, X.M.; Liao, W.J. Advances in the genetic regulating pathways of plant flowering time. *Biodivers. Sci.* **2021**, *29*, 825–842.
33. Taiz, L.; Zeiger, E. The control of flowering. In *Plant Physiology*, 5th ed.; Fosket, D.E., Amasino, R., Eds.; Sinauer Associates, Inc.: Sunderland, MA, USA, 2010.
34. Amasino, R.C. Vernalization and flowering time. *Curr. Opin. Biotechnol.* **2005**, *16*, 154–158.
35. Michaels, S.D.; Amasino, R.M. FLOWERING LOCUS C encodes a novel MADS domain protein that acts as a repressor of flowering. *Plant Cell* **1999**, *11*, 949–956.

36. Greb, T.; Mylne, J.S.; Crevillen, P.; Geraldo, N.; An, H.; Gendall, A.R.; Dean, C. The PHD finger protein VRN5 functions in the epigenetic silencing of *Arabidopsis FLC*. *Curr. Biol.* **2007**, *17*, 73–78.
37. Kim, D.H.; Sung, S. The plant homeo domain finger protein, VIN3-LIKE 2, is necessary for photoperiod-mediated epigenetic regulation of the floral repressor, MAF5. *Proc. Natl. Acad. Sci. USA* **2010**, *107*, 17029–17034.
38. Lucia, F.D.; Crevillen, P.; Jones, A.M.E.; Greb, T.; Dean, C. A PHD-polycomb repressive complex 2 triggers the epigenetic silencing of *FLC* during vernalization. *Proc. Natl. Acad. Sci. USA* **2008**, *105*, 16831–16836.
39. Sung, S.; Schmitz, R.J.; Amasino, R.M. A PHD finger protein involved in both the vernalization and photoperiod pathways in *Arabidopsis*. *Genes Dev.* **2006**, *20*, 3244–3248.
40. Levy, Y.Y.; Mesnage, S.; Mylne, J.S.; Gendall, A.R.; Dean, C. Multiple roles of *Arabidopsis* VRN1 in vernalization and flowering time control. *Science* **2002**, *297*, 243–246.
41. Baurle, I.; Smith, L.; Baulcombe, D.C.; Dean, C. Widespread role for the flowering-time regulators FCA and FPA in RNA-mediated chromatin silencing. *Science* **2007**, *318*, 109–112.
42. Hornyik, C.; Terzi, L.C.; Simpson, G.G. The spen family protein FPA controls alternative cleavage and polyadenylation of RNA. *Dev. Cell* **2010**, *18*, 203–213.
43. Schomburg, F.M.; Patton, D.A.; Meinke, D.W.; Amasino, R.M. *FPA*, a gene involved in floral induction in *Arabidopsis*, encodes a protein containing RNA-recognition motifs. *Plant Cell* **2001**, *13*, 1427–1436.
44. Ripoll, J.J.; Rodriguez-Cazorla, E.; Gonzalez-Reig, S.; Andujar, A.; Alonso-Cantabrana, H.; Perez-Amador, M.A.; Carbonell, J.; Martinez-Laborda, A.; Vera, A. Antagonistic interactions between *Arabidopsis* K-homology domain genes uncover *PEPPER* as a positive regulator of the central floral repressor *FLOWERING LOCUS C*. *Dev. Biol.* **2009**, *333*, 251–262.
45. Yamada, K.; Lim, J.; Dale, J.M.; Chen, H.; Shinn, P.; Palm, C.J.; Southwick, A.M.; Ecker, J.R. Empirical analysis of transcriptional activity in the *Arabidopsis* genome. *Science* **2003**, *302*, 842–846.
46. Henderson, I.R.; Liu, F.Q.; Drea, S.; Simpson, G.G.; Dean, C. An allelic series reveals essential roles for FY in plant development in addition to flowering-time control. *Development* **2005**, *132*, 3597–3607.
47. Simpson, G.G.; Dijkwel, P.P.; Quesada, V.; Henderson, I.; Dean, C. FY is an RNA 3' end-processing factor that interacts with FCA to control the *Arabidopsis* floral transition. *Cell* **2003**, *113*, 777–787.
48. Aukerman, M.J.; Lee, I.; Weigel, D.; Amasino, R.M. The *Arabidopsis* flowering-time gene *LUMINIDEPENDENS* is expressed primarily in regions of cell proliferation and encodes a nuclear protein that regulates *LEAFY* expression. *Plant J.* **1999**, *18*, 195–203.
49. Jiang, D.; Yang, W.; He, Y.; Amasino, R.M. *Arabidopsis* relatives of the human lysine-specific demethylase1 repress the expression of *FWA* and *FLOWERING LOCUS C* and thus promote the floral transition. *Plant Cell* **2007**, *19*, 2975–2987.
50. Liu, F.; Quesada, V.; Crevillen, P.; Baurle, I.; Swiezewski, S.; Dean, C. The *Arabidopsis* RNA-binding protein FCA requires a lysine-specific demethylase 1 homolog to downregulate *FLC*. *Mol. Cell* **2007**, *28*, 398–407.
51. Zemach, A.; Li, Y.; Ben-Meir, H.; Oliva, M.; Mosquna, A.; Kiss, V.; Avivi, Y.; Ohad, N.; Grafi, G. Different domains control the localization and mobility of LIKE HETEROCHROMATIN PROTEIN1 in *Arabidopsis* nuclei. *Plant Cell* **2006**, *18*, 133–145.
52. Upadhyya, R.; Lee, J.; Willis, I.M. Maf1 is an essential mediator of diverse signals that repress RNA polymerase III transcription. *Mol. Cell* **2002**, *10*, 1489–1494.
53. Park, S.; Oh, S.; Ek-Ramos, J.; van Nocker, S. *PLANT HOMOLOGOUS TO PARAFIBROMIN* is a component of the PAF1 complex and assists in regulating expression of genes within H3K27ME3-enriched chromatin. *Plant Physiol.* **2010**, *153*, 821–831.
54. Zhang, H.; van Nocker, S. The *VERNALIZATION INDEPENDENCE 4* gene encodes a novel regulator of *FLOWERING LOCUS C*. *Plant J.* **2002**, *31*, 663–673.
55. Pien, S.; Fleury, D.; Mylne, J.S.; Crevillen, P.; Inze, D.; Avramova, Z.; Dean, C.; Grossniklaus, U. *ARABIDOPSIS TRITHORAX1* dynamically regulates *FLOWERING LOCUS C* activation via histone 3 lysine 4 trimethylation. *Plant Cell* **2008**, *20*, 580–588.
56. Saleh, A.; Alvarez-Venegas, R.; Yilmaz, M.; Le, O.; Hou, G.C.; Sadder, M.; Al-Abdallat, A.; Xia, Y.N.; Lu, G.Q.; Ladunga, I.; et al. The highly similar *Arabidopsis* homologs of trithorax ATX1 and ATX2 encode proteins with divergent biochemical functions. *Plant Cell* **2008**, *20*, 568–579.
57. Shafiq, S.; Berr, A.; Shen, W.H. Combinatorial functions of diverse histone methylations in *Arabidopsis thaliana* flowering time regulation. *New Phytol.* **2014**, *201*, 312–322.
58. Deal, R.B.; Kandasamy, M.K.; McKinney, E.C.; Meagher, R.B. The nuclear actin-related protein ARP6 is a pleiotropic developmental regulator required for the maintenance of *FLOWERING LOCUS C* expression and repression of flowering in *Arabidopsis*. *Plant Cell* **2005**, *17*, 2633–2646.
59. Martin-Trillo, M.; Lazaro, A.; Poethig, R.S.; Gomez-Mena, C.; Pineiro, M.A.; Martinez-Zapater, J.M.; Jarillo, J.A. *EARLY IN SHORT DAYS 1 (ESD1)* encodes ACTIN-RELATED PROTEIN 6 (AtARP6), a putative component of chromatin remodelling complexes that positively regulates *FLC* accumulation in *Arabidopsis*. *Development* **2006**, *133*, 1241–1252.
60. March-Diaz, R.; Garcia-Dominguez, M.; Lozano-Juste, J.; Leon, J.; Florencio, F.J.; Reyes, J.C. Histone H2A.Z and homologues of components of the SWR1 complex are required to control immunity in *Arabidopsis*. *Plant J.* **2008**, *53*, 475–487.
61. Noh, Y.S.; Amasino, R.M. *PIE1*, an ISWI family gene, is required for *FLC* activation and floral repression in *Arabidopsis*. *Plant Cell* **2003**, *15*, 1671–1682.
62. Jiang, D.; Gu, X.; He, Y. Establishment of the winter-annual growth habit via *FRIGIDA*-mediated histone methylation at *FLOWERING LOCUS C* in *Arabidopsis*. *Plant Cell* **2009**, *21*, 1733–1746.

63. Choi, K.; Kim, J.; Hwang, H.J.; Kim, S.; Park, C.; Kim, S.Y.; Lee, I. The FRIGIDA complex activates transcription of *FLC*, a strong flowering repressor in *Arabidopsis*, by recruiting chromatin modification factors. *Plant Cell* **2011**, *23*, 289–303.
64. Schmitz, R.J.; Hong, L.; Michaels, S.; Amasino, R.M. *FRIGIDA-ESSENTIAL 1* interacts genetically with *FRIGIDA* and *FRIGIDA-LIKE 1* to promote the winter-annual habit of *Arabidopsis thaliana*. *Development* **2005**, *132*, 5471–5478.
65. Kim, S.Y.; Michaels, S.D. SUPPRESSOR OF FRI 4 encodes a nuclear-localized protein that is required for delayed flowering in winter-annual *Arabidopsis*. *Development* **2006**, *133*, 4699–4707.
66. Li, S.S.; Zhou, B.; Peng, X.B.; Kuang, Q.; Huang, X.L.; Yao, J.L.; Du, B.; Sun, M.X. *OsFIE2* plays an essential role in the regulation of rice vegetative and reproductive development. *New Phytol.* **2014**, *201*, 66–79.
67. Saleh, A.; Al-Abdallat, A.; Ndamukong, I.; Alvarez-Venegas, R.; Avramova, Z. The *Arabidopsis* homologs of trithorax (ATX1) and enhancer of zeste (CLF) establish ‘bivalent chromatin marks’ at the silent *AGAMOUS* locus. *Nucleic Acids Res.* **2007**, *35*, 6290–6296.
68. Ste-Marie, G.; Weinberger, P. Changes in carbohydrate metabolism in the wheat root tip after growth and vernalization. *Can. J. Bot.* **1971**, *49*, 195–200.
69. Avonce, N.; Leyman, B.; Thevelein, J.; Iturriaga, G. Trehalose metabolism and glucose sensing in plants. *Biochem. Soc. Trans.* **2005**, *33*, 276–279.
70. Gomez, L.D.; Baud, S.; Gilday, A.; Li, Y.; Graham, I.A. Delayed embryo development in the *ARABIDOPSIS TREHALOSE-6-PHOSPHATE SYNTHASE 1* mutant is associated with altered cell wall structure, decreased cell division and starch accumulation. *Plant J.* **2006**, *46*, 69–84.
71. Van Dijken, A.J.H.; Schluepmann, H.; Smeekens, S.C.M. *Arabidopsis* trehalose-6-phosphate synthase 1 is essential for normal vegetative growth and transition to flowering. *Plant Physiol.* **2004**, *135*, 969–977.
72. Angeles-Nunez, J.G.; Tiessen, A. *Arabidopsis* sucrose synthase 2 and 3 modulate metabolic homeostasis and direct carbon towards starch synthesis in developing seeds. *Planta* **2010**, *232*, 701–718.
73. Winter, H.; Huber, S.C. Regulation of sucrose metabolism in higher plants: Localization and regulation of activity of key enzymes. *Crit. Rev. Biochem. Mol. Biol.* **2000**, *35*, 253–289.
74. Levander, F.; Radstrom, P. Requirement for phosphoglucomutase in exopolysaccharide biosynthesis in glucose- and lactose-utilizing *Streptococcus thermophilus*. *Appl. Environ. Microb.* **2001**, *67*, 2734–2738.
75. Li, J.; Francisco, P.; Zhou, W.; Edner, C.; Steup, M.; Ritte, G.; Bond, C.S.; Smith, S.M. Catalytically-inactive β -amylase BAM4 required for starch breakdown in *Arabidopsis* leaves is a starch-binding-protein. *Arch. Biochem. Biophys.* **2009**, *489*, 92–98.
76. Griffiths, J.; Murase, K.; Rieu, I.; Zentella, R.; Zhang, Z.L.; Powers, S.J.; Gong, F.; Phillips, A.L.; Hedden, P.; Sun, T.P.; et al. Genetic characterization and functional analysis of the *GID1* gibberellin receptors in *Arabidopsis*. *Plant Cell* **2006**, *18*, 3399–3414.
77. Aukerman, M.J.; Sakai, H. Regulation of flowering time and floral organ identity by a microRNA and its *APETALA2*-like target genes. *Plant Cell* **2003**, *15*, 2730–2741.
78. Nakazawa, M.; Yabe, N.; Ichikawa, T.; Yamamoto, Y.Y.; Yoshizumi, T.; Hasunuma, K.; Matsui, M. *DFL1*, an auxin-responsive *GH3* gene homologue, negatively regulates shoot cell elongation and lateral root formation, and positively regulates the light response of hypocotyl length. *Plant J.* **2001**, *25*, 213–221.
79. Ugartechea-Chirino, Y.; Swarup, R.; Swarup, K.; Peret, B.; Whitworth, M.; Bennett, M.; Bougourd, S. The *AUX1 LAX* family of auxin influx carriers is required for the establishment of embryonic root cell organization in *Arabidopsis thaliana*. *Ann. Bot.* **2012**, *105*, 277–289.
80. Peret, B.; Swarup, K.; Ferguson, A.; Seth, M.; Yang, Y.; Dhondt, S.; James, N.; Casimiro, I.; Perry, P.; Syed, A.; et al. *AUX/LAX* genes encode a family of auxin influx transporters that perform distinct functions during *Arabidopsis* development. *Plant Cell* **2012**, *24*, 2874–2885.
81. Liscum, E.; Reed, J.W. Genetics of Aux/IAA and ARF action in plant growth and development. *Plant Mol. Biol.* **2002**, *49*, 387–400.
82. Ellis, C.M.; Nagpal, P.; Young, J.C.; Hagen, G.; Guilfoyle, T.J.; Reed, J.W. *AUXIN RESPONSE FACTOR1* and *AUXIN RESPONSE FACTOR2* regulate senescence and floral organ abscission in *Arabidopsis thaliana*. *Development* **2005**, *132*, 4563–4574.
83. Hagen, G.; Guilfoyle, T.J. Auxin-responsive gene expression: Genes, promoters and regulatory factors. *Plant Mol. Biol.* **2002**, *49*, 373–385.
84. Li, X.G.; Su, Y.H.; Zhao, X.Y.; Li, W.; Gao, X.Q.; Zhang, X.S. Cytokinin overproduction-caused alteration of flower development is partially mediated by *CUC2* and *CUC3* in *Arabidopsis*. *Gene* **2010**, *450*, 109–120.
85. Hwang, I.; Chen, H.C.; Sheen, J. Two-component signal transduction pathways in *Arabidopsis*. *Plant Physiol.* **2002**, *129*, 500–515.
86. Hwang, I.; Sheen, J. Two-component circuitry in *Arabidopsis* cytokinin signal transduction. *Nature* **2001**, *413*, 383–389.
87. Suárez-López, P.; Wheatley, K.; Robson, F.; Onouchi, H.; Valverde, F.; Coupland, G. *CONSTANS* mediates between the circadian clock and the control of flowering in *Arabidopsis*. *Nature* **2001**, *410*, 1116–1120.
88. Edwards, K.D.; Anderson, P.E.; Hall, A.; Salathia, N.S.; Locke, J.C.; Lynn, J.R.; Straume, M.; Smith, J.Q.; Millar, A.J. *FLOWERING LOCUS C* mediates natural variation in the high-temperature response of the *Arabidopsis* circadian clock. *Plant Cell* **2006**, *18*, 639–650.
89. Chow, B.Y.; Helfer, A.; Nusinow, D.A.; Kay, S.A. *ELF3* recruitment to the *PRR9* promoter requires other evening complex members in the *Arabidopsis* circadian clock. *Plant Signal. Behav.* **2012**, *7*, 170–173.
90. Liu, X.L.; Covington, M.F.; Fankhauser, C.; Chory, J.; Wagner, D.R. *ELF3* encodes a circadian clock-regulated nuclear protein that functions in an *Arabidopsis* *PHYB* signal transduction pathway. *Plant Cell* **2001**, *13*, 1293–1304.

91. Li, X.; Ma, D.; Lu, S.X.; Hu, X.; Huang, R.; Liang, T.; Xu, T.; Tobin, E.M.; Liu, H. Blue light- and low temperature-regulated COR27 and COR28 play roles in the *Arabidopsis* circadian clock. *Plant Cell* **2016**, *28*, 2755–2769.
92. Wang, P.; Cui, X.; Zhao, C.; Shi, L.; Zhang, G.; Sun, F.; Cao, X.; Yuan, L.; Xie, Q.; Xu, X. COR27 and COR28 encode nighttime repressors integrating *Arabidopsis* circadian clock and cold response. *J. Integr. Plant Biol.* **2017**, *59*, 78–85.
93. Liu, L.; Li, C.Y.; Song, S.Y.; Teo, Z.W.N.; Shen, L.S.; Wang, Y.W.; Jackson, D.; Yu, H. FTIP-dependent STM trafficking regulates shoot meristem development in *Arabidopsis*. *Cell Rep.* **2018**, *23*, 1879–1890.
94. Song, S.; Chen, Y.; Liu, L.; See, Y.H.B.; Mao, C.; Gan, Y.; Yu, H. OsFTIP7 determines auxin-mediated anther dehiscence in rice. *Nat. Plants* **2018**, *4*, 495–504.
95. Lee, J.; Oh, M.; Park, H.; Lee, I. SOC1 translocated to the nucleus by interaction with AGL24 directly regulates *LEAFY*. *Plant J.* **2008**, *55*, 832–843.
96. Adamczyk, B.J.; Fernandez, D.E. MIKC* MADS domain heterodimers are required for pollen maturation and tube growth in *Arabidopsis*. *Plant Physiol.* **2009**, *149*, 1713–1723.
97. Birkenbihl, R.P.; Jach, G.; Saedler, H.; Huijser, P. Functional dissection of the plant-specific SBP-domain: Overlap of the DNA-binding and nuclear localization domains. *J. Mol. Biol.* **2005**, *352*, 585–596.
98. Jofuku, K.D.; den Boer, B.G.W.; Van Montagu, M.; Okamoto, J.K. Control of *Arabidopsis* flower and seed development by the homeotic gene *APETALA2*. *Plant Cell* **1994**, *6*, 1211–1225.
99. Krizek, B.A. Ectopic expression of *AINTEGUMENTA* in *Arabidopsis* plants results in increased growth of floral organs. *Dev. Genet.* **1999**, *25*, 224–236.
100. Krogan, N.T.; Hogan, K.; Long, J.A. *APETALA2* negatively regulates multiple floral organ identity genes in *Arabidopsis* by recruiting the co-repressor TOPLESS and the histone deacetylase HDA19. *Development* **2012**, *139*, 4180–4190.
101. Nole-Wilson, S.; Tranby, T.L.; Krizek, B.A. *AINTEGUMENTA*-like (*AIL*) genes are expressed in young tissues and may specify meristematic or division-competent states. *Plant Mol. Biol.* **2005**, *57*, 613–628.
102. Castillejo, C.; Pelaz, S. The balance between CONSTANS and TEMPRANILLO activities determines *FT* expression to trigger flowering. *Curr. Biol.* **2008**, *18*, 1338–1343.
103. Finnegan, E.J.; Sheldon, C.C.; Jardinaud, F.; Peacock, W.J.; Dennis, E.S. A cluster of *Arabidopsis* genes with a coordinate response to an environmental stimulus. *Curr. Biol.* **2004**, *14*, 911–916.
104. Yoshida, S.; van der Schuren, A.; van Dop, M.; van Galen, L.; Saiga, S.; Adibi, M.; Moeller, B.; Ten Hove, C.A.; Marhavy, P.; Smith, R.; et al. A SOSEKI-based coordinate system interprets global polarity cues in *Arabidopsis*. *Nat. Plants* **2019**, *5*, 160–166.
105. van Dop, M.; Fiedler, M.; Mutte, S.; de Keijzer, J.; Olijslager, L.; Albrecht, C.; Liao, C.Y.; Janson, M.E.; Bienz, M.; Weijers, D. DIX domain polymerization drives assembly of plant cell polarity complexes. *Cell* **2020**, *180*, 427–439.e12.
106. Tian, X.; Wang, Z.; Li, X.; Lv, T.; Liu, H.; Wang, L.; Niu, H.; Bu, Q. Characterization and functional analysis of pyrabactin resistance-like abscisic acid receptor family in rice. *Rice* **2015**, *8*, 1–13.
107. Ashida, Y.; Yokobatake, N.; Kohchi, C.; Shimoda, K.; Hirata, T. Cloning of cDNA encoding ethylene-responsive element binding protein-5 in the cultured cells of *Nicotiana tabacum*. *DNA Seq.* **2000**, *11*, 125–129.
108. Zhu, L.; Liu, D.; Li, Y.; Li, N. Functional phosphoproteomic analysis reveals that a serine-62-phosphorylated isoform of ethylene response factor110 is involved in *Arabidopsis* bolting. *Plant Physiol.* **2013**, *161*, 904–917.
109. O'Malley, R.C.; Rodriguez, F.I.; Esch, J.J.; Binder, B.M.; O'Donnell, P.; Klee, H.J.; Bleecker, A.B. Ethylene-binding activity, gene expression levels, and receptor system output for ethylene receptor family members from *Arabidopsis* and tomato. *Plant J.* **2005**, *41*, 651–659.
110. Breton, G.; Danyluk, J.; Charron, J.B.F.; Sarhan, F. Expression profiling and bioinformatic analyses of a novel stress-regulated multispanning transmembrane protein family from cereals and *Arabidopsis*. *Plant Physiol.* **2003**, *132*, 64–74.
111. Liu, Z.; Jia, Y.; Ding, Y.; Shi, Y.; Li, Z.; Guo, Y.; Gong, Z.; Yang, S. Plasma membrane CRPK1-mediated phosphorylation of 14-3-3 proteins induces their nuclear import to fine-tune CBF signaling during cold response. *Mol. Cell* **2017**, *66*, 117–128.e5.
112. Meng, X.; Wang, H.; He, Y.; Liu, Y.; Walker, J.C.; Torii, K.U.; Zhang, S. A MAPK cascade downstream of *ERECTA* receptor-like protein kinase regulates *Arabidopsis* inflorescence architecture by promoting localized cell proliferation. *Plant Cell* **2012**, *24*, 4948–4960.
113. Wang, H.; Ngwenyama, N.; Liu, Y.; Walker, J.C.; Zhang, S. Stomatal development and patterning are regulated by environmentally responsive mitogen-activated protein kinases in *Arabidopsis*. *Plant Cell* **2007**, *19*, 63–73.
114. Yoshida, R.; Hobo, T.; Ichimura, K.; Mizoguchi, T.; Takahashi, F.; Aronso, J.; Ecker, J.R.; Shinozaki, K. ABA-activated SnRK2 protein kinase is required for dehydration stress signaling in *Arabidopsis*. *Plant Cell Physiol.* **2002**, *43*, 1473–1483.
115. Rodrigues, A.; Adamo, M.; Crozet, P.; Margalha, L.; Confraria, A.; Martinho, C.; Elias, A.; Rabissi, A.; Lumberras, V.; Gonzalez-Guzman, M.; et al. ABI1 and PP2CA phosphatases are negative regulators of Snf1-related protein kinase1 signaling in *Arabidopsis*. *Plant Cell* **2013**, *25*, 3871–3884.
116. Liu, X.; Zhu, Y.; Zhai, H.; Cai, H.; Ji, W.; Luo, X.; Li, J.; Bai, X. AtPP2CG1, a protein phosphatase 2C, positively regulates salt tolerance of *Arabidopsis* in abscisic acid-dependent manner. *Biochem. Biophys. Res. Commun.* **2012**, *422*, 710–715.
117. Yoshida, T.; Nishimura, N.; Kitahata, N.; Kuromori, T.; Ito, T.; Asami, T.; Shinozaki, K.; Hirayama, T. *ABA-hypersensitive germination3* encodes a protein phosphatase 2C (AtPP2CA) that strongly regulates abscisic acid signaling during germination among *Arabidopsis* protein phosphatase 2Cs. *Plant Physiol.* **2006**, *140*, 115–126.
118. Chern, M.; Bai, W.; Ruan, D.; Oh, T.; Chen, X.; Ronald, P.C. Interaction specificity and coexpression of rice NPR1 homologs 1 and 3 (NH1 and NH3), TGA transcription factors and negative regulator of resistance (NRR) proteins. *BMC Genom.* **2014**, *15*, 1–20.

-
119. Hirayama, T.; Shinozaki, K. A *cdc5+* homolog of a higher plant, *Arabidopsis thaliana*. *Proc. Natl. Acad. Sci. USA* **1996**, *93*, 13371–13376.
 120. Palma, K.; Zhao, Q.G.; Cheng, Y.T.; Bi, D.L.; Monaghan, J.; Cheng, W.; Zhang, Y.L.; Li, X. Regulation of plant innate immunity by three proteins in a complex conserved across the plant and animal kingdoms. *Genes Dev.* **2007**, *21*, 1484–1493.